



Effect of La and Mn on the properties of alkaline niobate-based piezoelectric ceramics

Henry E. Mgbemere & Gerold A. Schneider

To cite this article: Henry E. Mgbemere & Gerold A. Schneider (2016) Effect of La and Mn on the properties of alkaline niobate-based piezoelectric ceramics, *Journal of Asian Ceramic Societies*, 4:1, 97-101, DOI: [10.1016/j.jascer.2015.12.004](https://doi.org/10.1016/j.jascer.2015.12.004)

To link to this article: <https://doi.org/10.1016/j.jascer.2015.12.004>



© 2016 The Ceramic Society of Japan and
the Korean Ceramic Society



Published online: 20 Apr 2018.



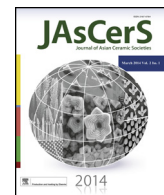
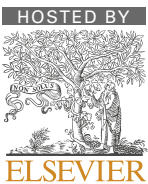
Submit your article to this journal



Article views: 15



View Crossmark data



Effect of La and Mn on the properties of alkaline niobate-based piezoelectric ceramics

Henry E. Mgbemere^{a,b,*}, Gerold A. Schneider^b

^a Department of Metallurgical & Materials Engineering, University of Lagos, Nigeria

^b Institute of Advanced Ceramics, Hamburg University of Technology, Denickestrasse 15, 21073, Hamburg, Germany



ARTICLE INFO

Article history:

Received 18 September 2015

Received in revised form

13 November 2015

Accepted 20 December 2015

Available online 7 January 2016

Keywords:

Ferroelectrics

Lead-free ceramics

(K_xNa_{1-x})NbO₃

Dopants

ABSTRACT

Lead-free ferroelectric (K_{0.44}Na_{0.52}Li_{0.04})(Nb_{0.86}Ta_{0.1}Sb_{0.04})O₃ ceramics co-doped with different amounts of both La and Mn have been produced using solid-state synthesis method. The relative density values of the unmodified sample are between 92 and 96% and decreases to ~91% for the sample with 1 mol% of the co-doping. Bi-modal grain distribution is observed in the samples while the average grain size decreases with co-doping due to grain growth inhibition by pinning of the grain boundary movement. The diffraction patterns show a transformation from an orthorhombic phase to a pseudo-tetragonal phase with co-dopants addition. The Curie temperature and the tetragonal-orthorhombic transition temperatures are lowered from ~9000 at 330 °C without modification to ~4000 at temperatures below 250 °C with co-dopant addition. The dielectric loss values of the samples also decrease from ~0.4 to 0.05 for temperatures up to 250 °C with co-doping. The remnant polarisation *P_r* of the samples decreases from ~8.55 kV/cm to ~6.57 kV/cm with co-dopant addition. The piezoelectric charge coefficient (*d₃₃*), including the normalised strain values, also decrease from ~400 pm/V and 220 pC/N to 157 pm/V and 159 pC/N, respectively with co-dopants up to 1 mol%.

© 2016 The Ceramic Society of Japan and the Korean Ceramic Society. Production and hosting by Elsevier B.V. This is an open access article under the CC BY-NC-ND license (<http://creativecommons.org/licenses/by-nc-nd/4.0/>).

1. Introduction

Lead zirconate titanate (Pb(Zr_xTi_{1-x})O₃ (PZT)) based piezoelectric ceramics finds a lot of application in actuators, sensors, transducers and other electromechanical devices because of their excellent piezoelectric properties and reliability in service. However, lead (Pb), which is one of the main constituent elements of these ceramics, is a toxic material, and when released to the atmosphere during ceramic processing, it causes both environmental and health problems, especially to children [1]. Another concern is the disposal of the waste lead in electronic devices after they have outlived their usefulness [2]. Legislations have been enacted by some multi-national governments like the European Commission banning its use in almost all products [3]. There is however no

overall suitable replacement yet for its use in piezoelectric ceramics, and so, it is still being allowed pending until a suitable replacement can be found.

The search for possible lead-free replacement compositions for PZT ceramics has more or less been focussed on (Bi_{0.5}Na_{0.5})TiO₃ [4–6] and (K_xNa_{1-x})NbO₃ [7–9] based ceramic systems and reports in the literature so far show that the later exhibits slightly higher piezoelectric properties but with lower temperature stability [2,10,11]. The research on KNN ceramics began in the late 1940s but was overtaken by PZT because of its better properties. A lot of research has been done on (K_xNa_{1-x})NbO₃ (KNN) based piezoelectric ceramics in the last 10 years accounting for more than 85% of all published works in the field [2,12]. Poor sintering and low piezoelectric properties are the main problems with pure KNN ceramics [13]. To overcome these problems, their ease of sintering and piezoelectric properties have been improved by substituting the main elements with dopants. Some of these combinations include KNN–Ba [14], KNN–SrTiO₃ [15,16], KNN–LiNbO₃ [17], KNN–LiTaO₃ [18], KNN–LiSbO₃ [19], (K,Na,Li)(Nb,Ta,Sb)O₃ [20] and pure KNN with sintering aids like CuO [21], ZnO [22], MnO₂ [23] and Bi₂O₃ [24].

The KNN-based ceramics modified with Li, Ta and Sb first reported by Saito et al. [20] remains one of the most studied

* Corresponding author.

E-mail addresses: h.mgbemere@unilag.edu.ng, henrymgbemere@yahoo.com (H.E. Mgbemere).

¹ The research work leading to this article was done while the first author was working at the Institute of Advanced Ceramics, Hamburg University of Technology, Hamburg Germany.

Peer review under responsibility of The Ceramic Society of Japan and the Korean Ceramic Society.

compositions in terms of piezoelectric charge coefficient (d_{33}) values and efforts are still being made by various researchers to improve on the existing values [25–27]. Manganese has been reported to improve the densification of KNN ceramics, suppress grain growth and helps to increase the electrical resistivity of the piezoceramic material, that is to improve resistivity [23,28,29]. Lanthanum has also been reported to improve the properties of PZT ceramics [30] and of BNT ceramics, provided it is <2 at.% [31,32]. Since the properties of BNT were improved on addition of La, it is also believed that it may have the same effect on KNN ceramics. Gao et al. studied the effect of Ce and La on KNN ceramics and reported that provided the doping amount is <1 mol%, the dielectric and ferroelectric properties values are maintained [33]. The effect of La_2O_3 on $(\text{K}_{0.5}\text{Na}_{0.5})(\text{Nb}_{0.96}\text{Sb}_{0.04})\text{O}_3$ showed that the grain size reduced, while the density, dielectric constant and piezoelectric coefficient values increased up to 0.6 mol% dopant addition [34]. BaTiO_3 has been co-doped with Mn and La in order to study their effects on the properties of the ceramics [35]. The authors want to determine the combined effects of two interesting dopants (La and Mn) on the properties of the well established $(\text{K}_{0.44}\text{Na}_{0.52}\text{Li}_{0.04})(\text{Nb}_{0.86}\text{Ta}_{0.1}\text{Sb}_{0.04})\text{O}_3$ ceramics. The objective therefore is to investigate the effects of co-doping on the structure, dielectric and piezoelectric properties of these ceramics.

2. Experimental procedure

The samples were synthesised using the mixed-oxide route from the following raw powders: K_2CO_3 , Na_2CO_3 , Li_2CO_3 (99+%), Sb_2O_3 , Nb_2O_5 , Ta_2O_5 (99.5%) (Chempur Feinchemikalien und Forschungs GmbH, Karlsruhe, Germany) and MnO_2 , La_2O_3 (99+) (Alfa Aesar GmbH, Karlsruhe, Germany). The raw powders were first dried in an oven for 4 h at a temperature of 220 °C to ensure that little or no moisture is present. Stoichiometric compositions of the powders were first weighed, mixed and attrition milled for 4 h using ethanol as solvent and 3 mm diameter ZrO_2 balls as the milling media. The ethanol was separated from the milled powder using a solvent extractor. Calcination of the milled powder was carried out at 750 °C for 4 h to ensure that the volatile components of the raw powders are removed so that the required composition $(\text{K}_{0.44}\text{Na}_{0.52}\text{Li}_{0.04})(\text{Nb}_{0.86}\text{Ta}_{0.1}\text{Sb}_{0.04})\text{O}_3$ is formed. It is believed that Sb_2O_3 being very unstable, readily oxidises from the +3 to the +5 valence state in the presence of air at elevated temperature to ensure stoichiometry. 0, 0.25, 0.5 and 1 mol% each of both La_2O_3 and MnO_2 raw powders were added to the sample and then the milling, solvent extraction and calcination steps were repeated to ensure that the powders are homogenous.

The powders were pressed into discs of 12.5 mm diameter and 4.5 mm initially with a uniaxial press operating at 40 MPa for 30 s and later with a cold isostatic press at 500 MPa for 2 min. The pellets were sintered in a chamber furnace at 1075 °C for 1 h with a heating and cooling rate of 3 °C/min and 10 °C/min, respectively. The density of the samples was determined using the Archimedes method while the crystal structure was examined using X-ray diffraction analysis with CuK_α radiation (D8 Discover, Bruker AXS Karlsruhe, Germany). Samples for microstructural examination were polished and thermally etched at 925 °C for 30 min. The microstructure was

observed using a scanning electron microscope (LEO 1530 SEM, Gemini/Zeiss, Oberkochen, Germany) while the grain size measurements were carried out using the mean intercept length method from at least six different areas of the image. A minimum of 100 grains was counted in the analysis of the average grain size.

Silver paints acting as electrodes were applied on both surfaces of the samples to be used for electrical measurements. The temperature dependence of the dielectric properties of the ceramics was measured from 20 Hz to 1 MHz with an LCR meter (HP 4284A, Agilent Technologies, Inc., Palo Alto, USA) attached to a heating furnace. The polarisation hysteresis curves were obtained using a standard Sawyer-Tower circuit while the strain hysteresis curves were obtained using an inductive transducer device. A complete hysteresis loop measurement was performed in 200 s. The piezoelectric coefficient d_{33} was measured using a low signal displacement transducer (Hottinger Baldwin Messtechnik GmbH, Darmstadt, Germany) connected to a lock-in amplifier while the slope of the strain hysteresis loop was used to obtain the high signal piezoelectric charge coefficient.

3. Results and discussion

The density values for the La and Mn co-doped $(\text{K}_{0.44}\text{Na}_{0.52}\text{Li}_{0.04})(\text{Nb}_{0.86}\text{Ta}_{0.1}\text{Sb}_{0.04})\text{O}_3$ ceramics are as shown in Table 1. A minimum of 12 samples was used in the calculation of the density values. The theoretical density values for the samples are also calculated using the X-ray diffraction patterns and it was assumed that the orthorhombic phase is the only phase present. In the unmodified sample, values ranging from 92% to 96% of the theoretical density are obtained. When La and Mn co-doping are introduced, the relative density value slightly decreases but the deviation from the mean density value also decreases. For the co-doped samples, the highest relative density value ($94.9 \pm 0.9\%$) is obtained with the sample modified with 0.5 mol% and decreases to $90.96 \pm 0.5\%$ with 1 mol%. Mn and La have been reported to improve the densification of piezoelectric ceramics through pinning of the grain boundary movement [28,34]. In this case, the co-dopants ensure that while the density value decreases, the deviation from the mean value of the density also decreases. The theoretical density values for each composition was calculated and it is 4.79 g/cm^3 for the unmodified sample and gradually increases to 4.84 g/cm^3 for the sample with 1 mol% co-doping.

The scanning electron microscope (SEM) images of the polished surface of the samples with different co-doping amounts are shown in Fig. 1. All the micrographs have grains with quasi-cubic morphology, which has been reported for KNN ceramics [36]. Grains that are relatively non-uniform in size and containing fewer amounts of pores are formed.

For the unmodified sample in Fig. 1a, an inhomogeneous grain size distribution can be observed. Some grains are very large relative to others and this abnormal grain growth leads to a bimodal grain size distribution with large grains being surrounded by smaller grains. Some of the smaller grains have sizes of as small as $\sim 600 \text{ nm}$. The average grain size for the large grains is $\sim 4.9 \pm 1.0 \mu\text{m}$, and for the small grains, it is $\sim 1.7 \pm 0.8 \mu\text{m}$. Unevenly distributed and sized pores can also be seen at the grain

Table 1

Data showing the density, dielectric and piezoelectric properties of $(\text{K}_{0.44}\text{Na}_{0.52}\text{Li}_{0.04})(\text{Nb}_{0.86}\text{Ta}_{0.1}\text{Sb}_{0.04})\text{O}_3$ ceramics co-doped with different amounts of La and Mn at room temperature.

Doping amount (mol%)	ε_r @ 1 kHz	$\tan \delta$ (1 kHz)	d_{33} (pC/N)	Normalised strain, d_{33}^* (pm/V)	Theoretical density (g/cm ³)	Relative density (%)	Remnant polarisation, P_r ($\mu\text{C}/\text{cm}^2$)	Coercive field, E_c (kV/cm)
0	~1146	0.1515	220	400 ± 10	4.79	94.25 ± 2.3	~18.9	8.55
0.25	~1397	0.0812	196	259 ± 5	4.81	93.87 ± 0.6	~10.0	6.57
0.5	~1311	0.0283	167	283 ± 5	4.82	94.87 ± 0.9	~10.0	6.57
1.0	~1357	0.0293	159	157 ± 4	4.84	90.96 ± 0.5	~7.5	6.57

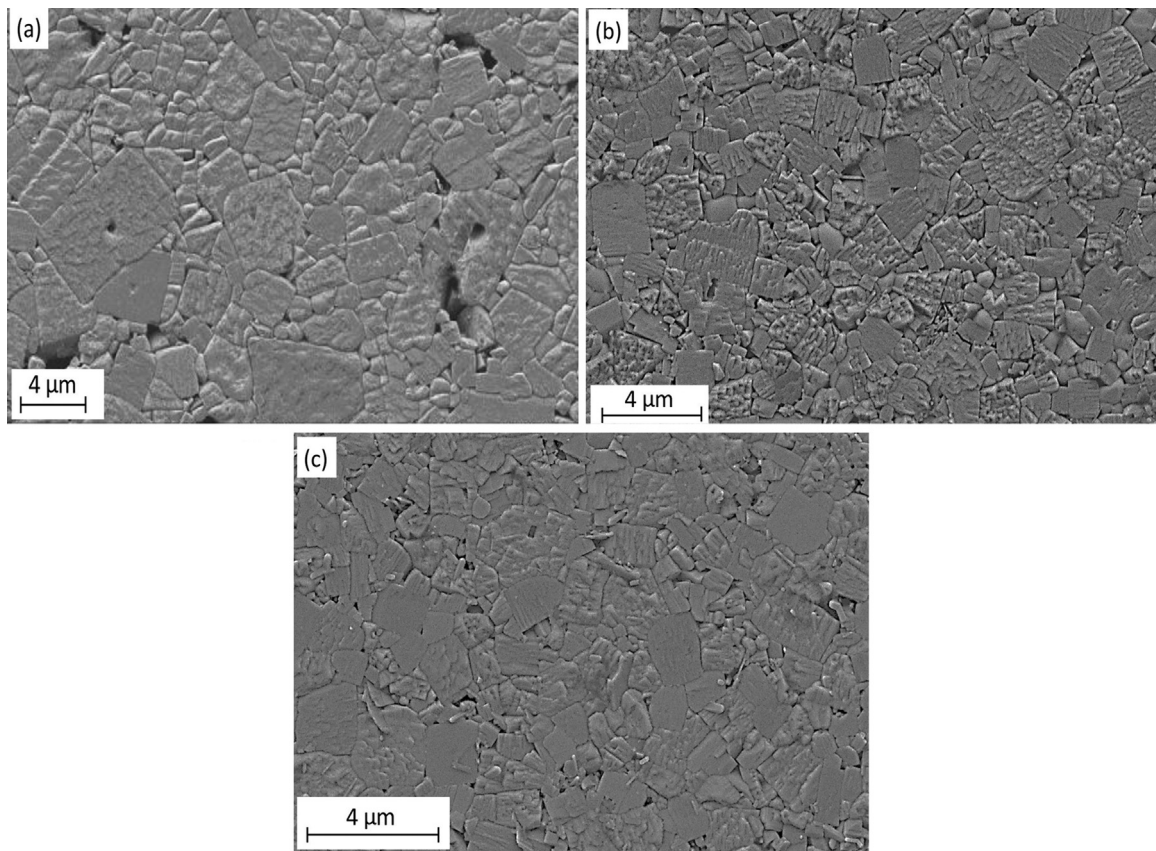


Fig. 1. Scanning electron microscope images of the thermally etched surfaces of $(\text{K}_{0.44}\text{Na}_{0.52}\text{Li}_{0.04})(\text{Nb}_{0.86}\text{Ta}_{0.1}\text{Sb}_{0.04})\text{O}_3$ ceramics sintered at 1075 °C for 1 h in air atmosphere showing (a) the undoped ceramic, (b) ceramic with 0.25 mol% of La, Mn and (c) with 0.5 mol% of La, Mn.

boundaries and there are also signs of liquid phase at the grain boundaries. Fig. 1b shows the microstructure of the sample with 0.25 mol% of the co-dopants. The surfaces of the samples have both smooth and rough grains, which may be attributed to the different crystallographic planes, which behave differently during etching. The higher energetic planes try to revert to the lower energetic planes and the result is a rough surface. It still has a bimodal grain size distribution but with fewer pores. The large grains have a mean grain size of $2.6 \pm 0.5 \mu\text{m}$ while the small grains have a mean grain size of $1.1 \pm 0.5 \mu\text{m}$. The microstructures of the samples co-doped with 0.5 mol% and 1 mol%, respectively are not significantly different and so only the sample with 0.5 mol% is presented. The amount of grains with large sizes continues to decrease such that the volume of grains with similar sizes increases. The large grains have an average particle size of $1.9 \pm 0.4 \mu\text{m}$ while the small grains have an average size of $0.8 \pm 0.4 \mu\text{m}$ (Fig. 1c). Mn is known to create oxygen vacancies in KNN ceramics, which hinders the movement of the grain boundaries and inhibits grain growth leading to lesser volume of pores in the microstructure [28,37]. In La-doped $(\text{Bi}_{0.5}\text{Na}_{0.5})\text{TiO}_3$ ceramics at 1 at.%, the grain size has been reported to increase [31].

Fig. 2 shows the X-ray diffraction (XRD) patterns for samples modified with different amounts of the dopants. The peak positions did not change significantly with doping but the peak shapes changed. In the unmodified state, the orthorhombic phase is the dominant structure at room temperature. There is a report in the literature that states that a two-phase orthorhombic/tetragonal coexistence is observed [38]. When 0.25 mol% of the co-dopant is added to the ceramic, the peak splitting between the orthorhombic and tetragonal phases at the Bragg angle of $\sim 47^\circ$ is roughly equal and indicates that the structure is close to the polymorphic phase boundary position. The volume of the tetragonal phase

gradually increases while that of the orthorhombic phase decreases with more dopant addition. A pseudocubic phase has been reported when there is La substitution on the A-site of the lattice [33]. Some extra peaks (marked with circles in Fig. 2) can be observed but could not be identified because its volume is very little in the extra peaks that were found. A second phase related to $\text{Na}_2\text{Ti}_4\text{O}_9$ has been reported when the A- and B-site of KNN ceramics has been simultaneously doped with La and Ti, respectively [39].

Fig. 3a shows the temperature dependence of the dielectric constant values measured on heating at 1 kHz for the sample co-doped

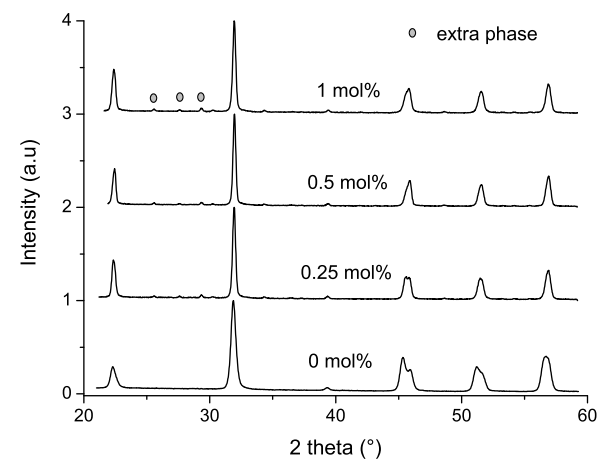


Fig. 2. X-ray diffraction patterns of $(\text{K}_{0.44}\text{Na}_{0.52}\text{Li}_{0.04})(\text{Nb}_{0.86}\text{Ta}_{0.1}\text{Sb}_{0.04})\text{O}_3$ ceramics doped with different amounts of dopants. Traces of an extra phase can be observed on the pattern containing 1 mol% of La and Mn.

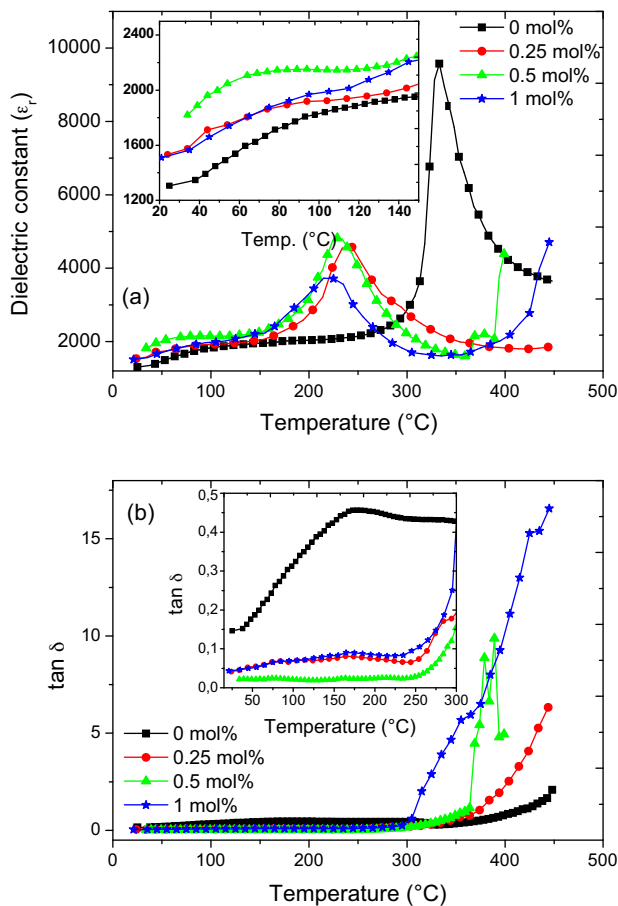


Fig. 3. Temperature dependence of (a) the dielectric constant values for $(\text{K}_{0.44}\text{Na}_{0.52}\text{Li}_{0.04})(\text{Nb}_{0.86}\text{Ta}_{0.1}\text{Sb}_{0.04})\text{O}_3$ ceramics measured at 1 kHz and (b) the dielectric loss ($\tan \delta$) values for $(\text{K}_{0.44}\text{Na}_{0.52}\text{Li}_{0.04})(\text{Nb}_{0.86}\text{Ta}_{0.1}\text{Sb}_{0.04})\text{O}_3$ ceramics measured at 1 kHz. The inset in the graph magnifies the region of the graph from 20 °C to 250 °C and from 20 °C to 300 °C for (a) and (b), respectively.

with different amount of La and Mn. There is a slight increase in the dielectric constant values at lower temperatures when the samples are modified with the dopants. Both phase transition temperatures (T_c and $T_{T.O.}$) decrease with increasing amount of the dopants. The T_c decreases from ~ 330 °C to ~ 240 °C when the dopants are added but do not decrease substantially with more additions. Addition of the dopants also led to a decrease in the dielectric constant values at the T_c . While a dielectric constant value of ~ 9000 was obtained in the sample without the dopants, 5000 and below is obtained in the doped samples at the T_c . Similar results have been reported for La_2O_3 and MnO_2 co-doped $0.02\text{Pb}(\text{Y}_{2/3}\text{W}_{1/3})\text{O}_3 - 0.98\text{Pb}(\text{Zr}_{0.52}\text{Ti}_{0.48})\text{O}_3$ [40]. Broadening at the dielectric constant peak is also observed for the doped samples. The higher the amount of doping used, the broader is the peak value at the T_c , which is an indication of possible relaxor behaviour.

The temperature dependence of the dielectric loss ($\tan \delta$) for the samples measured at 1 kHz is shown in Fig. 3b. The inset shows that at temperatures below 250 °C, the co-dopants are effective at reducing the loss behaviour of the ceramic. In the unmodified sample, the dielectric loss increases from 0.15 to ~ 0.45 as the measurement temperature increases. Addition of 0.25 mol% of the co-dopants led to a decrease in the loss values from ~ 0.4 to 0.05. Co-doping with 0.5 mol% gives the best result with values below 0.03 even at very high temperatures. Further addition up to 1 mol% increases the dielectric loss of the sample.

The polarisation hysteresis curves for the samples are shown in Fig. 4. All the measured samples attained saturation polarisation

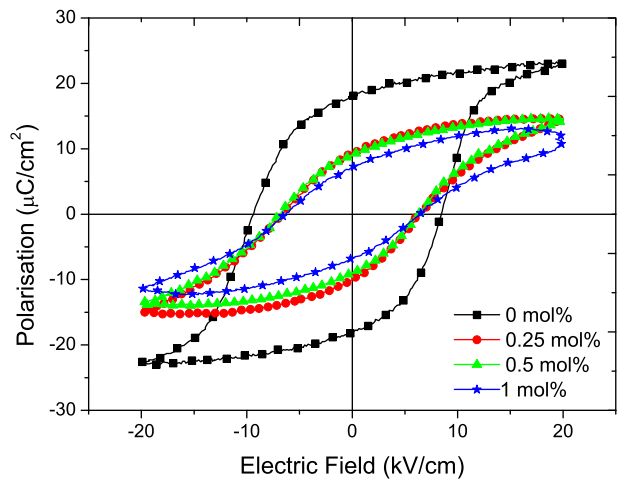


Fig. 4. A plot of the polarisation-electric field hysteresis curves for $(\text{K}_{0.44}\text{Na}_{0.52}\text{Li}_{0.04})(\text{Nb}_{0.86}\text{Ta}_{0.1}\text{Sb}_{0.04})\text{O}_3$ ceramics co-doped with different amounts of La and Mn.

when an electric field of 20 kV/cm is applied. The addition of the co-dopants to the ceramics led to a reduction in both the coercive field (E_c) and the remnant polarisation (P_r) values. In the sample with no modification, the P_r and E_c values are $\sim 18 \mu\text{C}/\text{cm}^2$ and $\sim 9 \text{kV}/\text{cm}$, respectively. Addition of 0.25 mol% each of the co-dopants led to a reduction in the P_r and E_c values to $\sim 10 \mu\text{C}/\text{cm}^2$ and $\sim 6.25 \text{kV}/\text{cm}$, respectively. With increasing dopant amounts, slightly reduced P_r values are obtained but there is no significant difference in the E_c values. The decrease in P_r values with increasing dopant amount is probably due to the pinning effect of the domain walls, which is a result of the increase in the number of defects in the lattice.

Fig. 5 shows the strain hysteresis curves for the ceramics modified with different amounts of the co-dopants. Samples with dopants up to 0.5 mol% could be measured and have the typical butterfly shape, which indicates the presence of ferroelectricity. Due to large leakage current, a good hysteresis curve could not be obtained for the sample modified with 1 mol% of the dopants. With increasing amount of the dopants, the area of the hysteresis loop decreases, which also agrees with their decreasing piezoelectric activity. The piezoelectric charge coefficient (d_{33}) values for the samples are shown in Table 1. The highest value of the normalised strain ($400 \pm 10 \text{ pm}/\text{V}$) is obtained in the unmodified sample. As the amount of co-dopants increases, the d_{33} value generally decreases

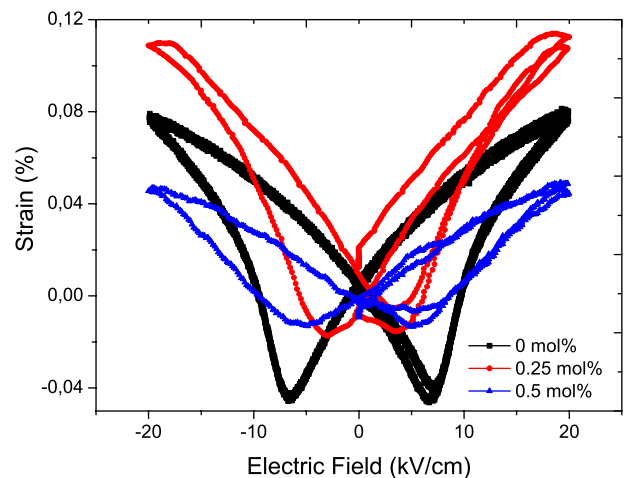
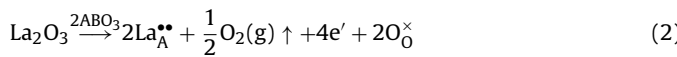


Fig. 5. A plot of the strain-electric field hysteresis curves for $(\text{K}_{0.44}\text{Na}_{0.52}\text{Li}_{0.04})(\text{Nb}_{0.86}\text{Ta}_{0.1}\text{Sb}_{0.04})\text{O}_3$ ceramics co-doped with different amounts of La and Mn.

but the reduction does not drastically change with the amounts of the dopants.

A possible explanation for the observed reduction in piezoelectric properties and increasing conductivity leading to dielectric breakdown in the samples with increasing amount of the co-dopants is given below. The ionic radius, valence state and coordination number of an ion is theoretically used to predict its position on the perovskite lattice. La³⁺ (1.06 Å) is believed to enter the A-site of the lattice since its size is closer to those of Na⁺ (1.02 Å) and K⁺ (1.39 Å). Mn, which is multi-valent in theory, and can enter both the A and B sites of the perovskite lattice. On the A-site of the lattice, the coordination number of K⁺, Na⁺ and Li⁺ is 12. La with a valence of +3, a coordination number of 12 and ionic radius of 1.06 Å, therefore, fits well into the A-site. On the B-site, Nb⁵⁺, Ta⁵⁺ and Sb⁵⁺ have coordination numbers of 6. Mn has different oxidation states and so its position in the perovskite lattice depends on its oxidation state. A current report in the literature on the state of Mn indicates that the possible state for it is predominantly +4 and sometimes +2 [29]. On the assumption that La will occupy the A-site position while Mn will occupy the B-site position of the perovskite lattice, La³⁺ on the A-site will create A-site vacancies whereas Mn will create oxygen vacancies as shown using the Kröger–Vink notation, as shown in Eqs. (1)–(3). With La³⁺ on the A-site of the lattice (Eq. (2)), it is also possible that oxygen gas will be liberated leading to the formation of electrons. Mn with a valence state of +4 will lead to the creation of oxygen vacancies in the perovskite lattice.



Simultaneous doping of the A and the B sites of the perovskite lattice can create internal bias field, which leads to the formation of defect dipoles. In a study of Bi_{0.5}Na_{0.5}TiO₃–Bi_{0.5}Li_{0.5}TiO₃–BaTiO₃ ceramics co-doped with La and Fe on the A and B sites respectively, it was reported that internal bias field was created, which led to the formation of defect dipoles of the type (Fe'_{Ti}–V_O[•]) [32]. This situation results in an asymmetric strain behaviour, which is observed in our work.

4. Conclusion

(K_{0.44}Na_{0.52}Li_{0.04})(Nb_{0.86}Ta_{0.1}Sb_{0.04})O₃ ceramics modified with different amounts of both La and Mn have been prepared using the conventional mixed-oxide method. The relative density values slightly decreased from 94.25 ± 2.3% in the unmodified sample to 91 ± 0.5% in the 1 mol% La and Mn sample. The degree of scatter in the doped samples is however lower. Bi-modal grain size distribution is observed in all the samples and the average grain size decreases with increasing co-dopant amounts. The crystal structure of the ceramics changed with co-dopant additions from a dominant orthorhombic phase through a two-phase orthorhombic-tetragonal coexistence to a pseudo-cubic phase with 1 mol%. The dielectric constant and dielectric loss values in the ceramics at lower temperatures improved when the dopants are added. The phase transition temperatures (T_c and T_{T-O}) in the ceramics are lowered with co-dopant additions but there is very little change in the transition temperatures with increasing amount of the dopants. The piezoelectric and ferroelectric properties of the ceramics decrease with dopant addition but no significant difference in the P_r and E_c values are observed with increasing amount

of the dopants. It is believed that the dopants being aliovalent to the unmodified composition, introduced cation, oxygen vacancies and defect dipoles into the perovskite lattice.

Acknowledgements

The research leading to these results has received financial support from Deutsche Forschungsgemeinschaft under grant no. SCHN 372/16-1.

References

- [1] H. Needleman, Annu. Rev. Med., 55, 209–222 (2004).
- [2] J. Rödel, K.G. Webber, R. Dittmer, W. Jo, M. Kimura and D. Damjanovic, J. Eur. Ceram. Soc., 35, 1659–1681 (2015).
- [3] European Parliament and the Council, Eur. J., 37, 1–9 (2003).
- [4] T. Takenaka and K. Sakata, Ferroelectrics, 95, 153–156 (1989).
- [5] T. Takenaka, K. Sakata and K. Toda, Ferroelectrics, 106, 375–380 (1990).
- [6] H.E. Mgbemere, R.P. Fernandes and G.A. Schneider, J. Eur. Ceram. Soc., 33, 3015–3022 (2013).
- [7] L. Egerton and D.M. Dillion, J. Am. Ceram. Soc., 42, 438–442 (1959).
- [8] J.-F. Li, K. Wang, F.-Y. Zhu, L.-Q. Cheng and F.-Z. Yao, J. Am. Ceram. Soc., 96, 3677–3696 (2013).
- [9] H.E. Mgbemere, M. Hinterstein and G.A. Schneider, J. Am. Ceram. Soc., 96, 201–208 (2013).
- [10] T.A. Skidmore, T.P. Comyn and S.J. Milne, Appl. Phys. Lett., 94, 222902 (2009).
- [11] E. Hollenstein, D. Damjanovic and N. Setter, J. Eur. Ceram. Soc., 27, 4093–4097 (2007).
- [12] J. Roedel, W. Jo, K.T.P. Seifert, E.-M. Anton, T. Granzow and D. Damjanovic, J. Am. Ceram. Soc., 92, 1153–1177 (2009).
- [13] H. Birol, D. Damjanovic and N. Setter, J. Eur. Ceram. Soc., 26, 861–866 (2006).
- [14] Z.S. Ahn and W.A. Schulze, J. Am. Ceram. Soc., 70, 18–21 (1987).
- [15] Y. Guo, K.-i. Kakimoto and H. Ohsato, Solid State Commun., 129, 279–284 (2004).
- [16] M. Kosec, V. Bobnar, M. Hrovat, J. Bernard, B. Malic and J. Holc, J. Mater. Res., 19, 1849–1854 (2004).
- [17] K.-i. Kakimoto, K. Akao, Y. Guo and H. Ohsato, Jpn. J. Appl. Phys., 44, 7064–7067 (2005).
- [18] E. Hollenstein, M. Davis, D. Damjanovic and N. Setter, Appl. Phys. Lett., 87, (2005).
- [19] G.-Z. Zang, J.-F. Wang, H.-C. Chen, W.-B. Su, C.-M. Wang, P. Qi, B.-Q. Ming, J. Du and L.-M. Zheng, Appl. Phys. Lett., 88, 212908 (2006).
- [20] Y. Saito, H. Takao, T. Tani, T. Nonoyama, K. Takatori, T. Homma, T. Nagaya and M. Nakamura, Nature, 432, 84–87 (2004).
- [21] M. Matsubara, K. Kikuta and S. Hirano, J. Appl. Phys., 97, 114105 (2005).
- [22] R. Chen and L. Li, J. Am. Ceram. Soc., 89, 2010–2015 (2006).
- [23] C.-W. Ahn, H.-C. Song, S. Nahm, S.-H. Park, K. Uchino, S. Priya, H.-G. Lee and K. Nam-Kee, Jpn. J. Appl. Phys., 44, L1361–L1364 (2005).
- [24] H. Du, D. Liu, F. Tang, D. Zhu and Z. Wancheng, J. Am. Ceram. Soc., 90, 2824–2829 (2007).
- [25] S.-Y. Choi, S.-J. Jeong, D.-S. Lee, M.-S. Kim, J.-S. Lee, J.H. Cho, B.I. Kim and Y. Ikuhara, Chem. Mater., 24, 3363–3369 (2012).
- [26] M.R. Bafandeh, R. Gharakhani and J.-S. Lee, J. Alloys Compd., 602, 285–289 (2014).
- [27] F.-Z. Yao, K. Wang, W. Jo, J.-S. Lee and J.-F. Li, J. Appl. Phys., 116, 114102 (2014).
- [28] H.E. Mgbemere, R.-P. Herber and G.A. Schneider, J. Eur. Ceram. Soc., 29, 1729–1733 (2009).
- [29] L. Wang, W. Ren, W. Ma, M. Liu, P. Shi and X. Wu, AIP Adv., 5, 097120 (2015).
- [30] M. Hammer and M.J. Hoffmann, J. Electroceram., 2, 75–84 (1998).
- [31] A. Herabut and A. Safari, J. Am. Ceram. Soc., 80, 2954–2958 (1997).
- [32] J. Li, F. Wang, C.M. Leung, S.W. Or, Y. Tang, X. Chen, T. Wang, X. Qin and W. Shi, J. Mater. Sci., 46, 5702–5708 (2011).
- [33] D. Gao, K.W. Kwok, D. Lin and H.L.W. Chan, J. Phys. D: Appl. Phys., 42, 035411 (2009).
- [34] J. Yoo and B. Seo, Ferroelectrics, 425, 106–113 (2011).
- [35] M.M.V. Petrović, J.D. Bobić, R. Grigalaitis, B.D. Stojanović and J. Banys, Acta Phys. Pol. A, 124, 155–160 (2013).
- [36] E. Ringgaard and T. Wurlitzer, J. Eur. Ceram. Soc., 25, 2701–2706 (2005).
- [37] L.-X. He and C.-E. Li, J. Mater. Sci., 35, 2477–2480 (2000).
- [38] H.E. Mgbemere, R.P. Fernandes, M. Hinterstein and G.A. Schneider, Z. Kristallogr., 226, 138–144 (2011).
- [39] J. Fuentes, J. Portelles, A. Pérez, M.D. Durruthy-Rodríguez, C. Ostos, O. Raymond, J. Heiras, M.P. Cruz and J.M. Siqueiros, Appl. Phys. A, 107, 733–738 (2012).
- [40] S.J. Yoon, S.Y. Yoo, J.H. Moon, H.J. Jung and H.J. Kim, J. Mater. Res., 11, 348–352 (1995).